Observation of the Linear Stark Effect in a Single Acceptor in Si

L. E. Calvet,[1,2,*] R. G. Wheeler,[2] and M. A. Reed[2]

[1]*Institut d'Electronique Fondamentale, Bâtiment 220, Université Paris-Sud, 91405 Orsay Cedex, France*
[2]*Departments of Applied Physics and Electrical Engineering, Yale University, New Haven, Connecticut 06520, USA*

(Received 22 March 2006; published 2 March 2007)

The Stark splitting of a single fourfold degenerate impurity located within the built-in potential of a metal-semiconductor contact is investigated using low temperature transport measurements. A model is developed and used to analyze transport as a function of temperature, bias voltage, and magnetic field. Our data is consistent with a boron impurity. We report g factors of $g_{1/2} = 1.14$ and $g_{3/2} = 1.72$ and a linear Stark splitting 2Δ of 0.1 meV.

DOI: 10.1103/PhysRevLett.98.096805 PACS numbers: 73.20.Hb, 71.55.Cn, 73.30.+y, 73.40.Gk

The investigation of single dopant atoms, or atomic-scale electronics, seeks to manipulate the charge and/or spin at the individual impurity level. Fundamentally, there is a deep analogy between natural atoms, typically studied in large ensembles using light and a single impurity confined in a semiconductor, measured by current transport [1]. The Stark effect has been explored in large ensembles of atoms [2,3], but an investigation of an individual confined impurity is lacking. Recent quantum computing proposals [4,5] make such explorations particularly relevant, especially those of single dopants in silicon situated in a complex environment [6,7]. Here we rely on traditional electron transport measurements of randomly placed shallow acceptors [8–11] and a novel geometry to explore the Stark splitting of an individual impurity.

In transport measurements involving a gate, changing V_g energetically moves a localized impurity level with respect to the contacts, and subsequent tunneling typically exhibits a Lorentzian spectral shape as it passes through the Fermi level. Here the gate is used to probe the energy position and conductance spectrum of the impurity and thus cannot be used to tune the Stark effect. The required low temperatures and equilibrium source-drain voltage necessary for observing single impurities are in apparent conflict with the high electric field one might apply perpendicular to the gate to probe such a perturbation. We resolve this by investigating a resonant impurity embedded in the built-in potential of a Schottky barrier and thus subject to a large electric field even at equilibrium.

The impurity is located near the metallic electrode of a Schottky barrier metal-oxide-semiconductor field-effect transistor (SBMOSFET) [12–16], in which the source and drain are made from the metallic silicide PtSi [as depicted in Fig. 1(a)]. At low temperatures and small bias voltages current transport is governed by direct tunneling through the Schottky barriers formed at the metal-semiconductor interface, whose resistance is much larger than that of the channel [14]. An acceptor impurity located near this interface modifies the potential V at the contact, enhances tunneling via its resonant level and is easily observable in low temperature transport measurements. We use a 1D model for $V(x)$ [15,16] that takes into account the perpendicular (z) electric field from the gate with the effective carrier concentration at the MOS surface, n_s. The total 1D potential $V(x)$ [Fig. 1(b)] includes a hydrogenic impurity and a standard metal-semiconductor depletion potential:

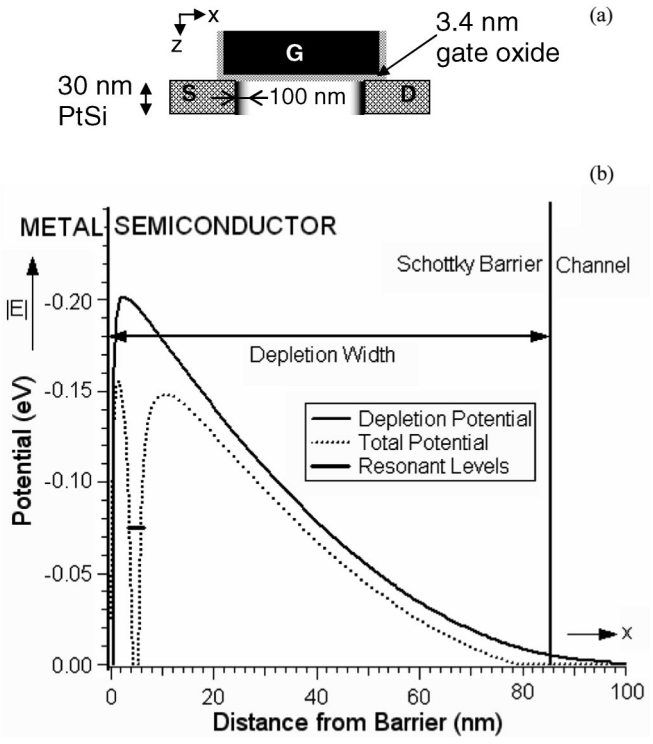

FIG. 1. (a) Schematic of the device. S, D, and G signify, respectively, the source, drain, and gate. The impurity (not shown) is located in the semiconductor near the metallic source or drain. A black and white contour plot of the depletion potential is drawn near the source and drain, where the scale ranges from 0.2 (black) to 0 (white) eV relative to the valence band. (b) The different potentials from the 1D model calculated using the parameters from Table I.

$$V(x) = -\frac{qN}{\varepsilon_s}\left(wx - \frac{x^2}{2}\right) + \varphi_{ib} - \frac{q}{4\pi\varepsilon_s|a-x|} - \frac{q}{16\pi\varepsilon_s x} + \frac{q}{16\pi\varepsilon_s(a+x)}, \quad (1)$$

where $w = \sqrt{\frac{2\varepsilon_s}{qn_s}\phi_{ib}}$ is the depletion width, a is the distance from the impurity to the metal, ϕ_{ib} is the SB height, and V_t is the threshold voltage. The last two terms in this equation are the image charge due to an electron tunneling through the potential and the charged acceptor. The SB height ($\phi_{ib} = 0.225$ eV) was determined from a fit to the thermionic emission equation in the 180–250 K range. The electric field $E_{\mathrm{SB}} = \frac{V(a-r_B)-V(a+r_B)}{2r_B}$, where r_B is the Bohr radius.

Acceptors in silicon have a fourfold degenerate ground state and belong to the Γ_8 representation. Here, the potential at the metal-semiconductor interface adds a large electric field across the impurity, potentially lifting the zero field fourfold degeneracy. We consider the linear Stark effect, which results in a splitting 2Δ for a field E applied parallel to the $\langle 100\rangle$ direction [7,17]:

$$\Delta = \pm|p_8|E, \quad (2)$$

where p_8 is the linear dipole moment of a Γ_8 level. In a magnetic field the impurity is mainly affected by the Zeeman effect, [17,18] with $\Delta E_z = E_{m_j} - E_{\mathrm{res}}(B=0) = g_{|m_j|}\mu_B m_j B$, where $m_j = +3/2, +1/2, -1/2$, and $-3/2$, for a magnetic field applied parallel to the $\langle 100\rangle$ direction. In addition to quadratic effects, the model neglects strain that may result from the PtSi source and drain.

The conductance of a resonant impurity is given by the Landauer formalism $G(E) = \frac{2e^2}{h}T(E)$. Here the transmission coefficient $T(E) = |t_+ + t_-|^2$, where $t_{x=+,-} = \frac{\sqrt{\Gamma_L^x\Gamma_R^x}}{(\Delta E \pm \Delta) + \frac{i\Gamma^x}{2}}$ are the probability amplitudes of the positive and negative Stark split levels, $\Gamma^x = \Gamma_L^x + \Gamma_R^x$ is the total leak rate of each Stark split peak, and $\Delta E = E - E_{\mathrm{res}}$ is the difference between the Fermi level and the zero field resonant level. When $2\Delta > \Gamma^x$ the conductance consists of two Lorentzian peaks located at $E = E_{\mathrm{res}} \pm \Delta$. At large enough temperatures ($\frac{\Gamma^+ + \Gamma^-}{2} + 2\Delta < 3.53k_BT$), the Stark split peaks experience a broadening due to the temperature dependence of the Fermi function [9,11,19].

The devices consist of an n-type polysilicon gate, a boron doped substrate (5×10^{21} m^{-3}), a 3.4 nm gate oxide, and 30 nm metal silicide PtSi regions as the source and drain [13]. Devices sizes were sufficiently small that individual impurities are easily identifiable and well separated. Because of the band bending at the SB the energetic position of impurities situated near the metal varies and resonances can be observed over a large range of gate bias.

Measurements were performed in a dilution refrigerator. Differential conductance dI/dV_{ds} was measured using a standard lock-in technique with V_{ds} applied in the $\langle 100\rangle$ direction. Characteristics were investigated as a function of temperature, bias voltage, and magnetic field. The magnetic field was applied perpendicular to the two-dimensional hole gas (2DHG) in the $\langle 001\rangle$ direction.

Figure 2(a) shows the dI/dV_{ds} versus V_g at different bias voltages. At $V_{\mathrm{ds}} = 0$ V, a splitting is clearly visible as the resonance exhibits a double peak with $2\Delta = V_{\mathrm{gres}}^+ - V_{\mathrm{gres}}^- = 0.6$ mV $= 0.1$ meV. The parameters from the zero bias Landauer fit are shown in Table I and indicate very asymmetric barriers. The fit is not unique since ${\Gamma_L}^x$ and ${\Gamma_R}^x$ are symmetric in $T(E)$; however, to observe the transport of a single impurity over that of the direct tunneling current (along the 20 μm device width), the impurity must be close to the metal. One striking characteristic at equilibrium is the peak height difference between the Stark split peaks. To understand this, we performed detailed simulations of the leak rates for a wide range of values of a and n_s using a WKB approximation (Ref. [20]):

$$\Gamma_0 = \hbar\omega_0\left\{\exp\left[-2\frac{1}{\hbar}\int_{x_0}^{x_L} dx(2m^*[V(x)-E])^{1/2}\right] + \exp\left[-2\frac{1}{\hbar}\int_{x_R}^{x_0} dx(2m^*[V(x)-E])^{1/2}\right]\right\}, \quad (3)$$

where ω_0 is the attempt frequency and $V(x)$ is given by Eq. (1). We find that the peak height difference cannot be explained by the difference in energy levels of the Stark split peaks. Instead, it is attributed to the anisotropy of the silicon bands near the impurity. In a traditional SB with image force, tunneling occurs within the semiconductor in the same energy band and thus m^* is the semiconductor effective mass in the direction of emission [21]. Here each level may be associated with a different effective mass. In addition m^* may be modified by quantization effects in the semiconductor channel.

Because of this anisotropy, one cannot determine a, n_s, and thus p_8 precisely. However, the 2 order magnitude difference in Γ_L and Γ_R is much more important than the factor of 2 difference in ${\Gamma_R}^+$ and ${\Gamma_R}^-$. We use the ratio of the right to left leak rates ($\sim$0.01) and the WKB simulations to find a range of n_s, corresponding to a unique a and p_8. To determine a lower bound, we use the 2D Silvaco simulator ATLAS$^{\mathrm{TM}}$ to find n_s at approximately 30 nm below the gate oxide, the approximate physical thickness of the source and drain. These results are summarized in Fig. 2(b) where p_8 ranges from 0.16–0.87 D.

Shallow boron acceptors are the most probable origin of the resonant states because the number of impurities in a device scales with its physical dimensions. The range of the linear dipole moment is reasonable compared with a previous experiment of an ensemble of boron impurities where $p_8 = 0.26 \pm 0.06$ D (Ref. [3]) and with theoretical effective mass approximation calculations of p_8 for B in Si that range from 0.9 D using a Coulomb potential to 6 D using a δ potential [3]. We note that variations in p_8 may arise from strain and local potential fluctuations surrounding the impurity.

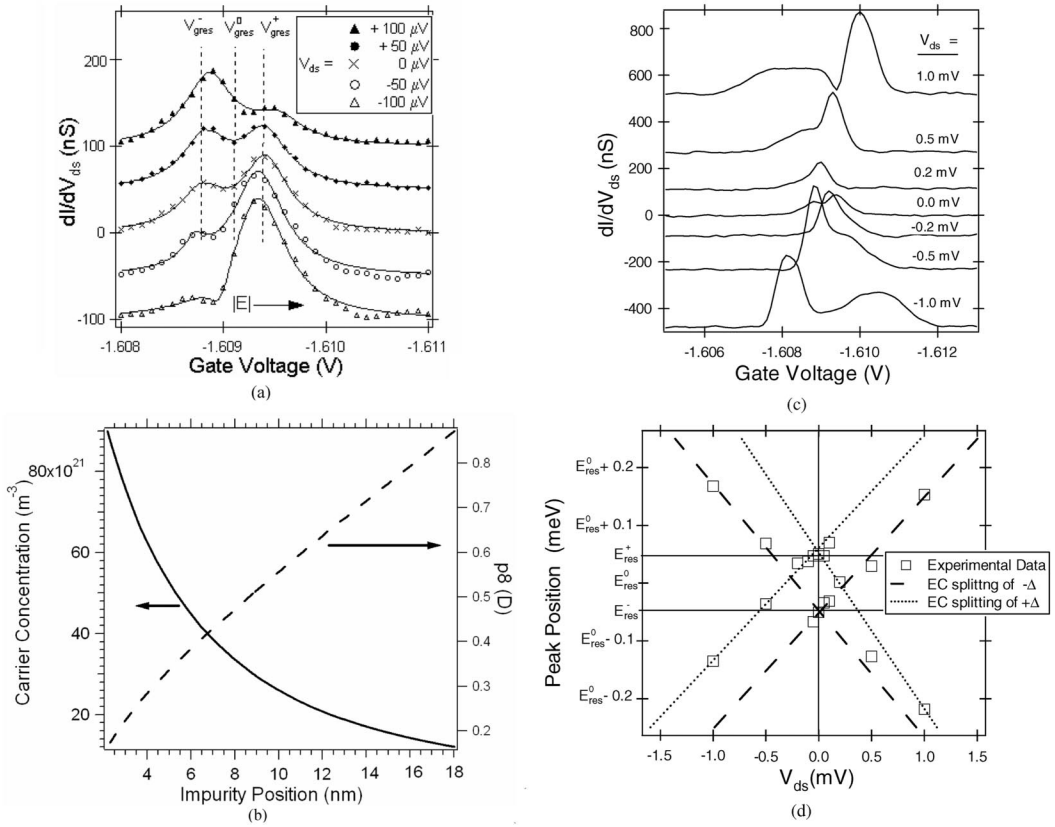

FIG. 2. (a) and (c) Differential conductance versus gate voltage for different bias voltages, at 50 mK. The $V_{ds} \neq 0$ curves are offset for clarity. The markers indicate the data and the solid lines are the fits. (b) The values obtained for n_s, a, and p_8 using Eqs. (1) and (3) and the parameters from Table I. The dipole moment is in debye (D) where 1 D $= 3.336 \times 10^{-30}$ Cm. (d) Peak position versus V_{ds} from (a) and (c). Note that $E^0_{res} = \alpha V_{gres}$, where $\alpha = 0.163$ eV/V is determined from the temperature dependence [19].

The nonequilibrium V_{ds} behavior is shown in Figs. 2(a) and 2(c). When V_{ds} is large enough that both Stark split peaks are in the transport window [Fig. 2(a)], both levels are active for conduction simultaneously; but each level cannot be simultaneously occupied because of the large Coulomb repulsion. Holes tunneling from the semiconductor ($V_{ds} \leq 0$) will tunnel through $\Gamma_R{}^+$ with greater probability and the positive Stark split peak dominates. Holes tunneling from the metal ($V_{ds} \geq 0$), are equally likely to tunnel onto the positive or negative Stark split peak; however, because they must wait a longer time to exit the dot via $\Gamma_R{}^-$, holes in this level limit the transport and thus dominate the current. In accordance with this interpretation, the peak height of the positive Stark split peak for $V_{ds} \leq 0$ is larger than its negative Stark split peak counterpart at positive bias.

As shown in Fig. 2(c), a similar effect is observed at larger bias. For a single resonance, one observes two peaks as the left and right electrochemical potential align with the resonant level, giving rise to a characteristic "X" in a plot of the dG/dV_g versus V_g as V_{ds} is varied. Here, a double X is expected, corresponding to the two Stark split levels. As above, however, one of the levels limits the current and thus dominates the conductance characteristics. For clarity, we plot in Fig. 2(d) the peak position of each resonance versus V_{ds} and the corresponding linear fits that show the outline of the double X.

To show unambiguously that the two resonant levels are associated with a single impurity (and are not, for instance, due to two spatially separated impurities each with a single resonant level), the magnetic field dependence is investigated. This data is best illustrated at $V_{ds} = 3$ mV [Fig. 3(a)], where at 0 T the $-\Delta$ level exhibits a sharp peak when $V^-_{gres}(V_{ds} \neq 0) > V^+_{gres}(V_{ds} = 0)$. This resonance has a large displacement towards higher energies until $\sim$1 T when it begins to decrease more gradually. We

TABLE I. Parameters used to obtain the linear dipole moment [Fig. 2(b)]. V^0_{gres} and Δ are obtained directly from the data and the leak rates from the fit to the Landauer equation.

V^0_{gres} (V)	2Δ (mV)	$\Gamma_L{}^+$ (10^{-4} V)	$\Gamma_L{}^-$ (10^{-4} V)	$\Gamma_R{}^+$ (10^{-6} V)	$\Gamma_R{}^-$ (10^{-6} V)
-1.6091	0.6	5.384 ± 0.23	5.047 ± 0.42	6.88 ± 0.49	3.36 ± 0.12

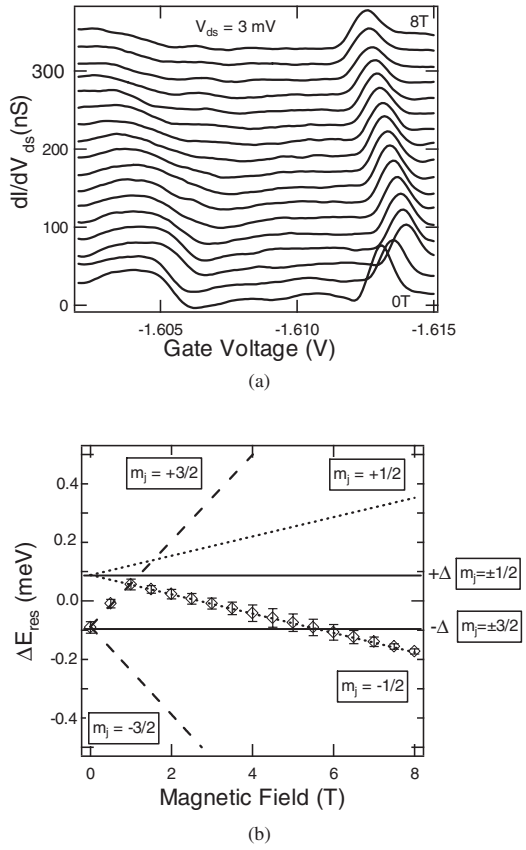

FIG. 3. (a) Differential conductance versus gate voltage as a function of magnetic field (in steps of 0.5 T). The B-0 curves are offset for clarity. (b) Identification of the m_j values for the Stark split levels. The data is plotted as circles with the errors indicating the standard deviation from a Lorentzian fit. The dashed and dotted lines indicate a linear regression of the peak positions.

identify the initial positive displacement as the motion of the $m_j = +3/2$ level and the subsequent negative displacement as that of the $m_j = -1/2$ level. This data set allows us to identify m_j of the Stark split levels and determine the g factors, as shown in Fig. 3(b), where $\Delta E^-_{\mathrm{res}}(B) = E^-_{\mathrm{res}}(B) - E^-_{\mathrm{res}}(0\ \mathrm{T})$ is plotted as a function of magnetic field B. A linear fit at $B \leq 1$ T reveals $g_{3/2} = 1.72 \pm 0.11$ and similarly for 1 T $\leq B \leq 8$ T results in $g_{1/2} = 1.14 \pm 0.02$. To compare these results with previous experimental research, we use the anisotropic model of Merlet *et al.* [22], [$g^{3/2}(100) = g'(1 + 9r)$, $g^{1/2}(100) = g'(1 + r)$], in which r is the deviation from spherical symmetry, and find $g' = 1.07$ and $r = 0.068$. Our results are consistent with previous experiments for boron impurities where $g' = 0.99$, $r = 0.013$. The difference in the r term is perhaps caused by the proximity of the impurity to the metallic interface.

We have demonstrated the Stark effect in the electron transport of a single impurity located near a metal-semiconductor interface in silicon. Our results are consistent with the dipole moment and g factor reported for an ensemble of boron impurities in the bulk silicon. The observed Stark splitting is at intermediate values compared to those mentioned in quantum computing proposals [5] considering acceptor impurities in silicon.

It is a great pleasure to thank C. Wang, J. P. Snyder, and J. R. Tucker for devices and helpful discussions. We acknowledge B. Reulet, A. Poon, K. Lehnert, R. Schoelkopf, and A. Kozhevnikov for experimental help and discussions. L. E. C. thanks CNRS for financial support and P. Levy and X. Waintal for invaluable insights. This work was funded in part by DARPA.

*Electronic address: lecalvet@aya.yale.edu

[1] M. A. Kastner, Phys. Today **46**, No. 1, 24 (1993).
[2] A. Ramdas and S. Rodriguez, Rep. Prog. Phys. **44**, 1297 (1981).
[3] A. Köpf and K. Lassman, Phys. Rev. Lett. **69**, 1580 (1992).
[4] B. E. Kane, Nature (London) **393**, 133 (1998).
[5] B. Golding and M. I. Dykman, cond-mat/0309147; B. A. Bernevig and S.-C. Zhang, Phys. Rev. B **71**, 035303 (2005).
[6] A. Fang, Y. C. Chang, and J. R. Tucker, Phys. Rev. B **66**, 155331 (2002); M. Friesen, Phys. Rev. Lett. **94**, 186403 (2005).
[7] G. D. J. Smit *et al.*, Phys. Rev. B **70**, 035206 (2004).
[8] A. B. Fowler *et al.*, Phys. Rev. Lett. **57**, 138 (1986).
[9] T. E. Kopley, P. L. McEuen, and R. G. Wheeler, Phys. Rev. Lett. **61**, 1654 (1988).
[10] M. W. Dellow *et al.*, Phys. Rev. Lett. **68**, 1754 (1992); J. W. Sakai *et al.*, Appl. Phys. Lett. **64**, 2563 (1994).
[11] M. R. Deshpande *et al.*, Phys. Rev. Lett. **76**, 1328 (1996); Phys. Rev. B **62**, 8240 (2000).
[12] J. R. Tucker, C. Wang, and P. Scott Carney, Appl. Phys. Lett. **65**, 618 (1994); J. M. Larson and J. P. Snyder, IEEE Trans. Electron Devices **53**, 1048 (2006).
[13] C. Wang, J. P. Snyder, and J. R. Tucker, Appl. Phys. Lett. **74**, 1174 (1999).
[14] L. E. Calvet, R. G. Wheeler, and M. A. Reed, Appl. Phys. Lett. **80**, 1761 (2002).
[15] L. E. Calvet *et al.*, Superlattices Microstruct. **28**, 501 (2000).
[16] R. A. Vega, IEEE Trans. Electron Devices **53**, 866 (2006); **53**, 1593 (2006).
[17] G. L. Bir, E. I. Butikov, and G. E. Pikus, J. Phys. Chem. Solids **24**, 1475 (1963); **24**, 1467 (1963).
[18] K. Suzuki, M. Okazaki, and H. Hasegawa, J. Phys. Soc. Jpn. **19**, 930 (1964).
[19] See EPAPS Document No. E-PRLTAO-98-058710 for a discussion of the temperature dependence. For more information about EPAPS, see http://www.aip.org/pubserv/epaps.html.
[20] M. Y. Azbel, Solid State Commun. **45**, 527 (1983).
[21] C. R. Crowell, Solid-State Electron. **12**, 55 (1969).
[22] F. Merlet *et al.*, Phys. Rev. B **12**, 3297 (1975).